

# The relationship between exercise-induced muscle fatigue, arterial blood flow and muscle perfusion after 56 days local muscle unloading

Tobias Weber<sup>1,2</sup>, Michel Ducos<sup>1,3</sup>, Edwin Mulder<sup>1</sup>, Åsa Beijer<sup>1,2</sup>, Frankyn Herrera<sup>1</sup>, Jochen Zange<sup>1</sup>, Hans Degens<sup>1,4</sup>, Wilhelm Bloch<sup>2</sup> and Jörn Rittweger<sup>1,4</sup>

<sup>1</sup>German Aerospace Center, Institute of Aerospace Medicine, Space Physiology, <sup>2</sup>Department of Molecular and Cellular Sport Medicine, <sup>3</sup>Institute of Biomechanics and Orthopaedics, German Sport University, Cologne, Germany, and <sup>4</sup>Institute for Biomedical Research into Human Movement and Health, Manchester Metropolitan University, Manchester, UK

## Summary

### Correspondence

Tobias Weber, German Aerospace Center, Institute of Aerospace Medicine, Space Physiology, Linder Höhe, 51147 Köln, Germany  
E-mail: tobias.weber@dlr.de

### Accepted for publication

Received 11 July 2013;  
accepted 06 September 2013

### Key words

arterial blood flow; muscle fatigue; muscle perfusion; muscle power; muscle unloading

In the light of the dynamic nature of habitual plantar flexor activity, we utilized an incremental isokinetic exercise test (IIET) to assess the work-related power deficit (WoRPD) as a measure for exercise-induced muscle fatigue before and after prolonged calf muscle unloading and in relation to arterial blood flow and muscle perfusion. Eleven male subjects ( $31 \pm 6$  years) wore the HEPHAISTOS unloading orthosis unilaterally for 56 days. It allows habitual ambulation while greatly reducing plantar flexor activity and torque production. Endpoint measurements encompassed arterial blood flow, measured in the femoral artery using Doppler ultrasound, oxygenation of the soleus muscle assessed by near-infrared spectroscopy, lactate concentrations determined in capillary blood and muscle activity using soleus muscle surface electromyography. Furthermore, soleus muscle biopsies were taken to investigate morphological muscle changes. After the intervention, maximal isokinetic torque was reduced by  $23.4 \pm 8.2\%$  ( $P < 0.001$ ) and soleus fibre size was reduced by  $8.5 \pm 13\%$  ( $P = 0.016$ ). However, WoRPD remained unaffected as indicated by an unchanged loss of relative plantar flexor power between pre- and postexperiments ( $P = 0.88$ ). Blood flow, tissue oxygenation, lactate concentrations and EMG median frequency kinematics during the exercise test were comparable before and after the intervention, whereas the increase of RMS in response to IIET was less following the intervention ( $P = 0.03$ ). In conclusion, following submaximal isokinetic muscle work exercise-induced muscle fatigue is unaffected after prolonged local muscle unloading. The observation that arterial blood flow was maintained may underlie the unchanged fatigability.

## Introduction

Disuse-induced adaptations of skeletal muscle are manifold. Not only is there muscle atrophy and a fibre-type shift towards more glycolytic type II fibres with a lower endurance capacity (Trappe et al., 2004; Degens & Alway, 2006), but there are also changes in electromyographic activity (Mulder et al., 2007) as well as distinct structural and functional adaptations of blood vessels supplying the unloaded muscles (Thijssen et al., 2010).

As blood vessels are able to rapidly adjust to altered functional demands and considering that peripheral blood flow is

dependent on the vasculature, adaptations of structure and function of blood vessels that reduce blood flow must be considered to limit the ability to perform on-going muscle contractions and thus to increase exercise-induced muscle fatigability. Muscle fatigue is a general phenomenon that has been previously assessed in different ways (Enoka & Duchateau, 2008) and partly explainable as a result of the above adaptations, muscle performance in terms of maximal force output and exercise-induced muscle fatigue has indeed been found to be impaired after prolonged disuse (Mulder et al., 2007). The disuse-induced increase of muscle fatigue is, however, not unequivocal, as various studies have found no

effect (Witzmann et al., 1983; Koryak, 1996) or even a decreased fatigability (Semmler et al., 2000; Shaffer et al., 2000) after muscle unloading. Some parts of the discrepancies between studies may be related to different models of disuse, investigated parameters and exercise protocols. In addition, exercise-induced muscle fatigue as studied in previous research (Koryak, 1996; Portero et al., 1996; Semmler et al., 2000; Mulder et al., 2007) was predominantly investigated performing sustained isometric contractions where blood flow is already occluded at comparably low torque levels (de Ruiter et al., 2007) or performing intermittent isometric contractions (Witzmann et al., 1983; Koryak, 1996; Mulder et al., 2007). These studies did not consider the dynamic nature of the majority of daily locomotive muscle contractions. Other human studies have investigated exercise-induced muscle fatigue under dynamic conditions after disuse did not investigate parameters for arterial blood supply and muscle perfusion (Berg et al., 1993; Deschenes et al., 2002) and final conclusions about the specific impact of blood supply on changes of exercise-induced muscle fatigue under dynamic conditions after periods of muscle disuse cannot be made.

Consequently, for the purpose of the present work, it should be investigated in how dynamic contractions and moderate work rate would affect muscular power generation after prolonged local muscle unloading. Local exercise-induced fatigue was thus assessed calculating the work-related power deficit (WoRPD) during a standardized local exercise test. This test was specifically developed to reflect habitual calf muscle contractions where a steady blood supply allows for enduring muscle work.

Yet, if reductions in blood supply to locomotive muscles during muscle disuse contribute to dynamic exercise intolerance, this holds great clinical potential to develop effective preventive measures in disease and injury rehabilitation in conditions associated with muscle unloading, aiming at maintaining local circulation (e.g. low-intensity exercise or thermotherapy). Therefore, the aim of the present study was to investigate the relationship between blood supply and isokinetic WoRPD after a period of local muscle unloading. Local disuse adaptations in calf muscle blood supply and WoRPD were studied using the HEPHAISTOS unloading orthosis that greatly reduces calf muscle force production during the stance phase without altering the gait pattern (Weber et al., 2013; Ducos M, Weber T, Albracht K, Brüggemann G-P, Rittweger J, manuscript in revision). Previous whole body (Huonker et al., 2003; Bleeker et al., 2005b; De Groot et al., 2006) and local disuse studies (Shaffer et al., 2000; Sugawara et al., 2004; Bleeker et al., 2005a) have found that the vasculature adapts distinctly, structurally as well as functionally to unloading. However, these studies did not elaborate on the consequences of the disuse-induced vascular adaptations with regard to exercise-induced muscle fatigue in terms of a WoRPD.

It was in the light of the above considerations the aim of the present study to comprehensively investigate changes of local blood supply and its potential impact on

exercise-induced muscle fatigue after prolonged muscle unloading. In order to investigate the functional muscle capacity during an incremental isokinetic exercise test (IIET) that was performed before and after the unloading intervention, isokinetic plantar flexor torque was continuously recorded and muscle power was calculated. Further, neuronal changes after muscle unloading should be detected measuring electromyographic soleus muscle activity during the exercise test, while femoral artery blood flow (ultrasonography), blood lactate concentrations and soleus muscle tissue oxygenation (near-infrared spectroscopy) were measured to assess changes of blood supply and metabolic properties of the unloaded muscle. In addition, before and after the HEPHAISTOS intervention, muscle biopsies were taken from the soleus muscle and histochemically analysed to assess fibre-type distribution and muscle capillarization.

Thus, the primary hypothesis of the present study was that after 8 weeks of local muscle unloading, the local blood flow at a given relative submaximal workload is reduced. We further expected a priori that if blood flow would be reduced, the reduction of blood supply would lead to an increase of WoRPD under isokinetic conditions.

## Methods

### Participants

Before study inclusion, subjects underwent comprehensive medical and psychological examinations. Prior to commencement of the study, a written informed consent was obtained from all subjects. The HEPHAISTOS study was approved by the Ethics Committee of the Northern Rhine medical association (Ärztchamber Nordrhein, Duesseldorf, Germany).

### Procedures

#### Unloading orthosis

In order to inactivate the calf muscles during locomotion, subjects wore the HEPHAISTOS orthosis in all daily activities that required loading of the legs (Fig. 1, patent application number 102011082700.5). The orthosis allows normal ambulation while activation and force production of the major calf muscles are significantly reduced, whereas the impact of ground reaction forces is completely retained. The biomechanical principles and acute effects of wearing the HEPHAISTOS are published elsewhere (Ducos M, Weber T, Albracht K, Brüggemann G-P, Rittweger J, manuscript in revision). In short, HEPHAISTOS reduces the plantar lever arm of the foot by approximately 35%, while ground reaction forces are retained. This leads to a substantial reduction of plantar flexor activation and plantar flexor torque production, in particular of the soleus muscle. A natural gait pattern can be maintained through the function of the elastic foot underneath the sole, which stores and releases energy during gait much like the



**Figure 1** HEPHAISTOS. A subject wearing the HEPHAISTOS unloading orthosis and the elevated contralateral plateau shoe.

Achilles tendon. The link below leads to the DLR Space Physiology webpage where a video of a subject walking with HEPHAISTOS is presented ([http://www.dlr.de/me/en/desktopdefault.aspx/tabid-7389/12432\\_read-35410/](http://www.dlr.de/me/en/desktopdefault.aspx/tabid-7389/12432_read-35410/)).

### HEPHAISTOS intervention

A detailed description of the study design of the HEPHAISTOS intervention will be published elsewhere (Weber et al., manuscript in revision). The study has been registered at [www.clinicaltrials.gov](http://www.clinicaltrials.gov) (NCT01576081). Briefly, the HEPHAISTOS study (HEP-study) was conducted as an integrative single-group ambulatory interventional study. Eleven healthy male subjects ( $31 \pm 6$  years) wore the HEPHAISTOS unloading orthosis unilaterally for 56 days, while on the other leg, a shoe with an elevated sole of the same height was worn. During the study, participants visited the laboratory for measurements and reports on a weekly basis.

### Isokinetic incremental exercise test

An exercise test was performed at baseline data collection (BDC) and on the last day of the intervention (HEP56) that

was thought to be challenging, but not impossible to complete after 56 days HEPHAISTOS unloading. An incremental exercise design was chosen to ensure valid ultrasound measurements during the moderate stages in order to test the primary hypothesis and to enforce a work-related power deficit following the higher increments in order to test the secondary hypothesis. To allow investigations of WoRPD characteristics independently of changes related to maximal strength losses, submaximal target torque stages were normalized to the current maximal voluntary contraction (MVC) strength. While lying in supine position with the foot attached to a dynamometer (Biodex system 3; Biodex Medical Systems, Shirley, NY, USA), subjects performed four incremental exercise stages that were, based on pilot study results, set to 30%, 40%, 45% and 50% of the current isokinetic maximum voluntary contraction strength (MVC<sub>R</sub>), which in turn was assessed prior to the exercise test. Each stage consisted of 40 submaximal contractions, followed by two maximal isokinetic plantar flexor contractions. Foot dorsiflexion was performed passively with external support. Between successive stages, subjects rested for an interval of 5 s. Angular velocity was set to  $20 \text{ deg s}^{-1}$  and the total movement angle ranged from  $-5 \text{ deg}$  dorsiflexion to  $15 \text{ deg}$  plantar flexion, where  $0 \text{ deg}$  refers to the neutral position. To assess the reference MVC (MVC<sub>R</sub>), subjects performed two sets of five maximal contractions per set, with 1-min pause between sets. The incremental submaximal stages were then set as a fraction of the MVC<sub>R</sub>. During the IIET, subjects performed two MVCs before the first stage and two MVCs at the end of each stage. The highest power of the two MVCs at the end of a stage was used to assess WoRPD, given as a percentage power difference from MVC<sub>R</sub>. For all MVC assessments, subjects were asked to produce as much plantar flexor torque as possible during verbal encouragement. Real-time visual feedback of the produced torque was provided to ascertain correct contraction strength for each submaximal stage. A schematic overview of the exercise protocol, including all measurements, is depicted in Fig. 2.

### Functional measurements

#### Isokinetic measurements

Plantar flexor torque ( $\tau$ ) was recorded during the entire exercise protocol using the internal software of the Biodex3 dynamometer and a sampling frequency of 100 Hz. Peak torques were then determined offline for each MVC. Angular velocity ( $\omega$ ) was set to  $20 \text{ deg s}^{-1}$  ( $0.3491 \text{ rad s}^{-1}$ ) for all torque measurements, and mechanical power ( $P$ ) was then calculated as:  $P = \tau \cdot \omega$ , with  $\tau$  in Nm and  $\omega$  in  $\text{rad s}^{-1}$  and  $P$  in  $\text{Nm s}^{-1}$ .

#### Arterial blood flow

Blood flow (BF) was measured in the superficial femoral artery (SFA) using a Doppler ultrasound device (Mylab 25; Esaote, Firenze, Italy) with a 7.5 to 12 MHz broadband linear

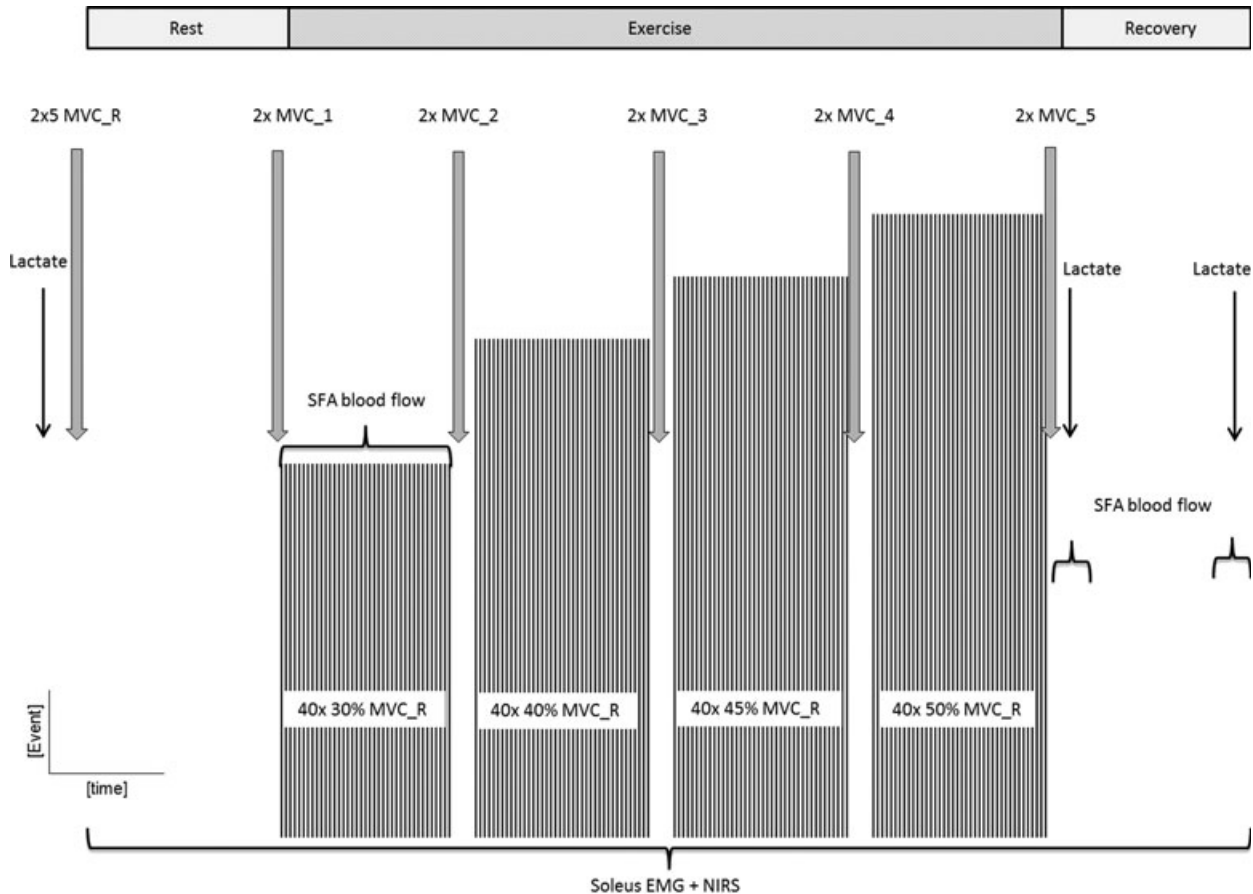


**Figure 2** Exercise protocol. Schematic overview of the isokinetic incremental exercise test (IET) including all measurements that were performed. MVC, maximal voluntary contraction; SFA, superficial femoral artery; EMG, electromyography; NIRS, near-infrared spectroscopy.

transducer. Resting blood flow ( $BF_{rest}$ ) was measured in the morning under standardized conditions: subjects were asked to fast, refrain from alcohol, caffeine and exercise for  $\geq 8$  h prior to the measurement. Throughout the IET, blood flow was measured during the 30% exercise stage ( $BF_{exercise}$ ), directly after the last stage of the protocol ( $BF_{rec1}$ ) and after 2 min of recovery ( $BF_{rec2}$ ). The Duplex mode was used to simultaneously measure arterial diameter and blood flow velocity. The angle of inclination for Doppler measurements was set to 60 deg where the probe was placed parallel to the longitudinal section of the artery. Ultrasound videos were recorded on an external computer using the analogue output of the device and a video-grabbing system (GrabsterAV 450MX; Terratec, Nettetal, Germany) together with an analogue to digital transformation software (MAGIX; Terratec, Nettetal, Germany). Offline analysis of the recorded videos was performed applying custom-built software (Bremser et al., 2012). Arterial blood flow was calculated using the envelope of the Doppler signal and the corresponding SFA diameters. Mean flow velocity ( $V_{mean}$ ) and the corresponding artery diameter ( $D$ ) were then used to calculate blood flow for each condition as:  $BF = \pi (D \cdot 0.5)^2 \cdot (V_{mean} \cdot 0.5) \cdot 60$ , with BF in  $ml \cdot min^{-1}$ ,  $V_{mean}$  in  $cm \cdot s^{-1}$  and  $D$  in cm. Exercise-induced dilation was calculated as the relative diameter increase from rest.

### Blood supply/mechanical power ratio

The blood flow values ( $ml \cdot min^{-1}$ ) for the 30% MVC stage ( $BF_{exercise}$ ) and the corresponding submaximal plantar flexor power ( $Nm \cdot s^{-1}$ ) were taken to calculate the ratio of blood supply and mechanical power (BF/P), with BF/P in  $ml \cdot Nm^{-1}$ .

### Muscle tissue oxygenation

Near-infrared spectroscopy was used during the entire experiment using a custom-made device (RheinAhrCampus Remagen of the Koblenz University of Applied Sciences). This device consists of a slow scan camera (model 7358-0003; Princeton Instruments, Roper Scientific, Trenton, NJ, USA), a detector chip with  $1340 \times 400$  pixels and 16 bit resolution, a controller unit (model Spec-10; Princeton Instruments, Roper Scientific) and a spectrometer (model SP-150; Acton optics and coatings; Princeton Instruments, Trenton, NJ, USA). Details about the mode of operation of this device have been published elsewhere (Geraskin et al., 2009). Tissue oxygenation index (TOI) was measured at the distal medial side of the soleus muscle using a sampling rate of 1 Hz. The median soleus muscle TOI was determined from data acquired 1 min before the IET ( $TOI_{rest}$ ) and for 2 min after the IET

(TOI<sub>recovery</sub>). The minimal TOI was determined using the full period of the incremental test (TOI<sub>exercise</sub>).

### Electromyography

Soleus muscle surface EMG was obtained using a telemetric device (Trigno Wireless; Delsys Inc., Boston, MA, USA) applying the Seniam recommendations for surface electromyography ([www.seniam.org](http://www.seniam.org)). Electromyographic recordings were obtained throughout the entire IET protocol using a sampling frequency of 4000 Hz. The signal was offline rectified and high pass-filtered (>50 Hz) with MATLAB (Mathworks, Natick, MA, USA). Submaximal contractions were detected by applying a threshold equivalent to 30 times the standard deviation of the EMG signal at rest. After visual inspection of the signal, incorrectly detected contractions were not considered. Subsequently, root mean square (RMS) and median frequency (MF) were calculated for each submaximal contraction. Values for RMS and MF of missing contractions were interpolated using the Piecewise Cubic Hermite Interpolating Polynomial (pChip function, MATLAB library). Means of RMS and MF were then calculated for all IET stages (Fig. 7).

### Lactate measurements

Blood lactate concentration was assessed in capillary blood taken from the ear lobe before, directly after and 2 min after the IET protocol (LA<sub>rest</sub>, LA<sub>rec1</sub>, LA<sub>rec2</sub>, respectively). The lactate concentration was analysed using a portable lactate analyser (Lactate Pro; Arkray, Kyoto City, Japan).

### Histochemical analysis

#### Biopsy sampling

Biopsy samples from soleus muscle were collected after overnight fasting, both at baseline and on the 50th day of the immobilization phase in order to assure uncompromised functional data acquisition at HEP56. Biopsies were taken from the lateral side of the muscle, approximately 1 cm below the belly of the lateral gastrocnemius muscle. After skin disinfection and local anaesthesia (2–3 ml of 2% Lidocaine), skin and muscle fasciae were incised for 10 mm and muscle samples were taken with a Weil–Blakely rongeur (Gebrüder Zepf Medizintechnik, Tuttlingen, Germany). Samples were, under rapid shaking, immediately frozen in liquid nitrogen and subsequently stored at –80°C for further analyses.

#### Lectin staining of capillaries

Ten-µm thick cross-sections of soleus muscle biopsies were cut in a cryostat. Capillaries were stained with lectin (*Ulex Europaeus*): sections were fixed in ice-cold acetone for 15 min and washed in HEPES buffer. Natural occurring peroxidase activity was blocked, and after washing in HEPES, sections were incubated

in lectin solution (50 µg ml<sup>-1</sup> in HEPES). The location of the capillaries was revealed with 40 min ABC-staining solution (ABC, Vectastain; Vector Laboratories, Burlingame, CA, USA) followed after wash steps, by incubation with DAB (DAB substrate kit; Vector Laboratories) and embedded in glycerine gelatine.

#### Myosin ATPase staining

Serial sections were stained for myosin ATPase according to Brooke & Kaiser (1970). Briefly, sections were preincubated in sodium acetate solution (pH: 4.35), washed, incubated in alkaline buffer (pH: 9.4), washed, incubated in cobalt chloride solution (2%), washed, incubated in ammonium sulphide solution (1%), washed and mounted in glycerine gelatine. Type I fibres appear dark and type II fibres light (Fig. 3).

#### Analysis of stained sections

Whole sections were photographed with a 20-fold magnification using a light microscope (Axio Scope.A1; Carl Zeiss Microscopy GmbH, Göttingen, Germany) and a USB-Monochrome camera with a 1280 × 960 pixel chip (ICX205AL; Sony Corporation, Tokyo, Japan). Lectin-stained images were then analysed using the custom-made 'HISTOMETER' software (Fig. 3), which is implemented as plugin into the IMAGEJ image processing software (ImageJ 1.46r; National Institute of Health, Bethesda, MD, USA). Regions of interest (ROIs) were determined in the area of the muscle section with predominantly polygonal or circular-shaped muscle fibres. Fibres that were sectioned longitudinally were avoided in the analysis. Based on pixel analyses within a given ROI smallest fibre diameters (DiaMin), fibre cross-sectional areas (FCSA), capillaries around fibres (CaF), capillary density (CD) and capillary-to-fibre ratio (C/F) were determined. DiaMin was calculated as the smallest diameter (in µm) of each fibre polygon that crosses the polygon centre of gravity (Fig. 3), FCSA was calculated as the sum of all pixels within one polygon (in µm<sup>2</sup>), CaF was calculated as the number of capillaries that were in direct contact with the fibre polygon (distance from capillary to fibre <9.3 µm), CD as the overall number of capillaries divided by the area of the entire ROI and C/F was calculated as the overall number of capillaries divided by the overall number of fibres. Finally, fibre-type distribution was assessed as the relative distribution of type I and type II fibres, and fibre area distribution as the relative area occupied by either fibre type. The average number of analysed fibres per ROI and section was 135 (SD = 48). All image analyses were performed by the same investigator.

#### Statistical analysis

Statistical analyses were performed using STATISTICA 8.0 for Windows (Statsoft, Tulsa, Oklahoma, USA, 1984–2008). A repeated-measures ANOVA was performed with four time levels (rest, exercise, rec1 and rec2) and two groups (BDC,

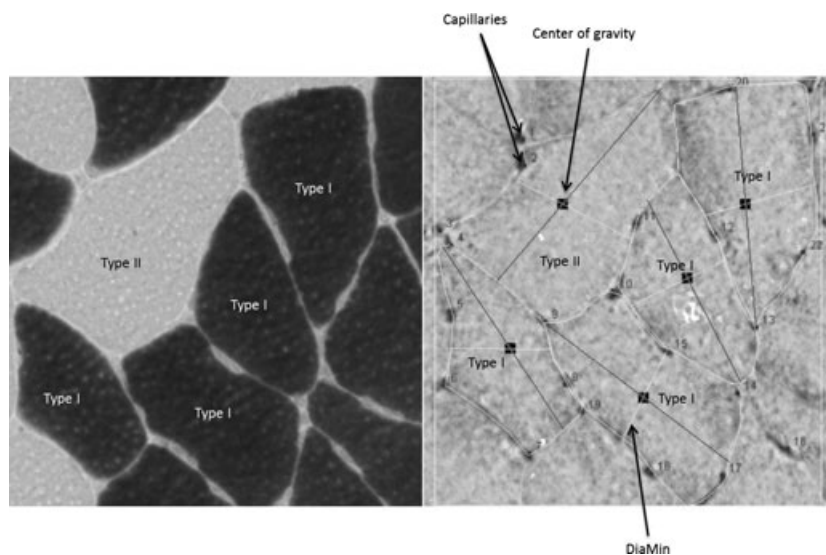


**Figure 3** Soleus muscle sections. Left: myosin ATPase staining. Right: lectin staining for capillaries. Fibre types were transferred from myosin ATPase sections. Fibre polygons and capillaries were then analysed using custom-built software. Numbers are assigned for each object by the software. Note that for each muscle fibre DiaMin crosses the polygon centre of gravity.

HEP56) to detect changes in arterial blood flow and exercising blood flow velocity. Exercise-induced dilation was tested in the same way with three different time levels (exercise, rec1 and rec2). Soleus muscle oxygenation ( $TOI_{rest}$ ,  $TOI_{exercise}$ ,  $TOI_{recovery}$ ) and lactate concentrations ( $LA_{rest}$ ,  $LA_{rec1}$ ,  $LA_{rec2}$ ) were analysed with three different time levels and two groups (BDC, HEP56). In order to assess changes of MVCs within the IIET protocol, a repeated-measures ANOVA was performed with six time levels (MVC<sub>R</sub>–MVC<sub>5</sub>) and two groups (BDC and HEP56). Electromyography data were analysed with four time levels (EMG<sub>30%MVC</sub>, EMG<sub>40%MVC</sub>, EMG<sub>45%MVC</sub> and EMG<sub>50%MVC</sub>) and two groups (BDC and HEP56). Tukey's test was used for post hoc testing. Pre-post-differences BF/P ratios as well as soleus muscle biopsy data were analysed with paired *t*-tests. Values are expressed as means  $\pm$  SD. The significance level was set at  $P \leq 0.05$ .

## Results

Due to reasons unrelated to the HEPHAISTOS intervention, one subject could not attend the HEP56 IIET. Nonetheless, soleus muscle biopsies of this subject were taken as scheduled and the data were taken into account for soleus muscle morphology analysis. Electromyography data of two subjects had to be discarded from analysis due to technical failure. Superficial femoral artery blood flow could only be measured at rest, during the moderate 30% MVC stage of the IIET and after the IIET and not, as it was initially planned and tested before on experienced investigators, during the entire IIET. Whole body motion artefacts generally precluded sufficient Duplex ultrasound measurements with the relatively inexperienced subjects during higher torque levels.

### Calf muscle performance

Absolute reference plantar flexor MVC torque (MVC<sub>R</sub>) was significantly ( $P < 0.001$ ) reduced by 23.4% (SD = 8.2%) at

HEP56 compared with the BDC value (Fig. 4a). During the IIET, MVC power declined significantly (time:  $P < 0.001$ ) from 49.9  $Nm s^{-1}$  (SD = 6.8  $Nm s^{-1}$ ) to 36.8  $Nm s^{-1}$  (SD = 6.7  $Nm s^{-1}$ ) at BDC and from 38.3  $Nm s^{-1}$  (SD = 6.9  $Nm s^{-1}$ ) to 27.2  $Nm s^{-1}$  (SD = 4.8  $Nm s^{-1}$ ) at HEP56 (Fig. 4b). The IIET-related power reductions on both days were comparable when expressed as per cent decline (group:  $P = 0.88$ ; Fig. 4c).

### Arterial blood flow parameters

Blood flow increased significantly in response to the IIET (time:  $P < 0.001$ ) from 96  $ml min^{-1}$  (SD = 27  $ml min^{-1}$ ) at rest ( $BF_{rest}$ ) to 250  $ml min^{-1}$  (SD =  $ml min^{-1}$ ) for  $BF_{exercise}$  and to 364  $ml min^{-1}$  (SD =  $ml min^{-1}$ ) until  $BF_{rec2}$ , that is, 2 min after termination of the IIET. Absolute SFA blood flow did not change after the intervention for any of the four tested time levels (Fig. 5a), as indicated by the absence of a significant group effect ( $P = 0.95$ ). Mean SFA blood flow velocity increased significantly in response to the IIET (Fig. 5b; time:  $P < 0.001$ ) with no significant differences between BDC and HEP56 (group:  $P = 0.16$ ). Resting and exercising SFA diameters were significantly smaller at HEP56 (Fig. 5b; group:  $P = 0.03$ ) compared with BDC. In response to the IIET, SFA diameter dilated significantly (time:  $P = 0.002$ ) by 5.8% (SD = 7.5%) from rest to 2 min recovery (rec2) for the pooled data of BDC and HEP56. There is trend (group:  $P = 0.07$ ) that HEP56 exercise dilation was more pronounced than BDC exercise dilation.

### Blood supply/mechanical power ratio

The ratio between SFA blood flow during the 30% MVC stage and the corresponding plantar flexor power (BF/P) increased significantly ( $P = 0.0046$ ) from 0.27  $ml Nm^{-1}$  (SD = 0.06  $ml Nm^{-1}$ ) at BDC to 0.39  $ml Nm^{-1}$  (SD = 0.11  $ml Nm^{-1}$ ) at HEP56 (Fig. 5d).

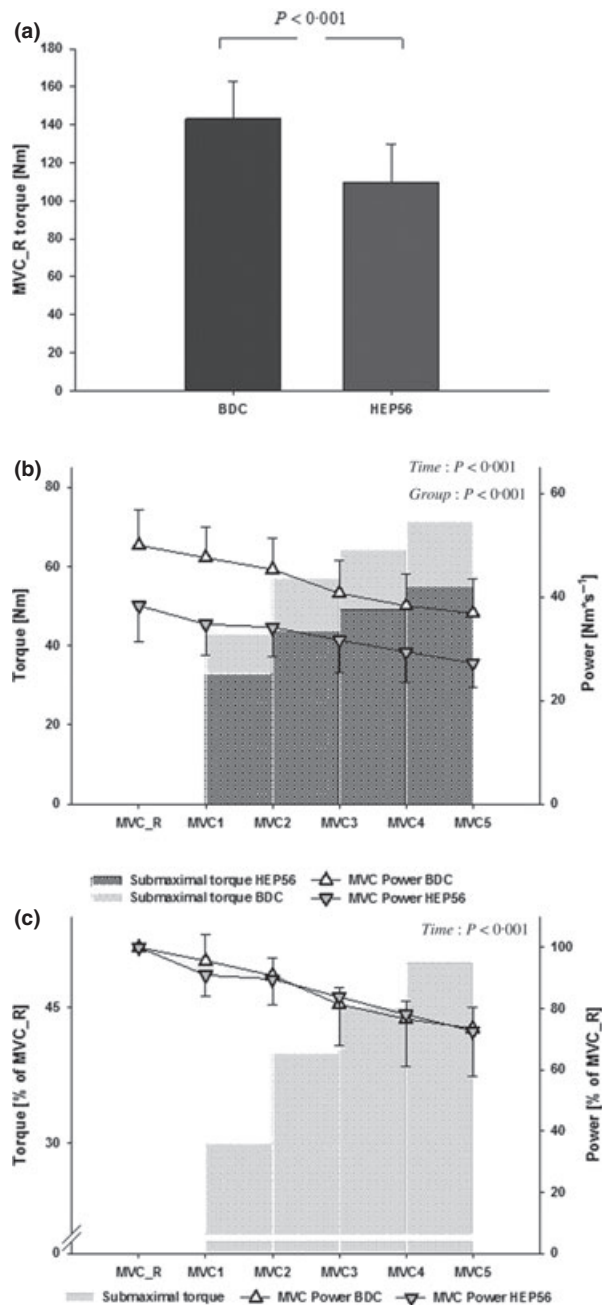


**Figure 4** Isokinetic plantar flexor performance. Panel (a) depicts the significant ( $P < 0.001$ ) decrease of 23.4% ( $SD = 8.2\%$ ) of absolute peak isokinetic plantar flexor torque (MVC\_R) after the intervention. The work-related power deficit is depicted in absolute values (b) and as percentage decrease from MVC\_R (c). Vertical bars depict submaximal work stages with the corresponding target torques; with MVC\_R as reference MVC and MVC1 to MVC5 as MVCs within the IET. There was no difference of the WoRPD between BDC and HEP56 ( $P = 0.88$ ).

### Soleus muscle tissue oxygenation

Soleus muscle TOI was not significantly different during the IET at HEP56 compared with BDC (group:  $P = 0.65$ ). In response to the IET, soleus muscle TOI decreased significantly

(time:  $P < 0.001$ ) from 55.8% ( $SD = 2.9\%$ ) at rest ( $TOI_{rest}$ ) to 50.8% ( $SD = 5.2\%$ ) during the IET ( $TOI_{exercise}$ ) and returned to baseline (56.0%;  $SD = 2.8\%$ ) during the 2 min recovery phase ( $TOI_{recovery}$ ; Fig. 6).

### Electromyography

In response to the IET, soleus muscle EMG MF decreased significantly (time:  $P = 0.04$ ) from 111 Hz ( $SD = 28$  Hz) during the 30% MVC stage to 101 Hz ( $SD = 15$  Hz) during the 50% MVC stage. There is a trend (group:  $P = 0.06$ ) that overall MFs were reduced after the intervention; however, the decrease in response to the IET was comparable between BDC and HEP56 (group\*time:  $P = 0.81$ ). The amplitude of the EMG signal increased significantly in response to the IET as indicated by an increased RMS throughout the experiment (time:  $P < 0.001$ ). The increase of RMS by 109% ( $SD = 68\%$ ) from the 30% MVC stage to the 50% MVC stage in response to the BDC IET appeared to be significantly more pronounced compared with the 67% ( $SD = 57\%$ ) increase in response to the HEP56 IET (group\*time = 0.03; Fig. 7).

### Lactate concentration

There was no difference between BDC and HEP56 capillary blood lactate concentration (group:  $P = 0.13$ ). In response to the IET, lactate concentration increased significantly (time:  $P < 0.001$ ) from 1.3 mmol l<sup>-1</sup> ( $SD = \text{mmol l}^{-1}$ ) at rest to 2.2 mmol l<sup>-1</sup> ( $SD = 0.59$  mmol l<sup>-1</sup>) directly after the IET and to 2.3 mmol l<sup>-1</sup> ( $SD = 0.62$  mmol l<sup>-1</sup>) 2 min after the IET.

### Soleus muscle morphology

Across fibre types, fibre size (DiaMin) was significantly ( $P = 0.016$ ) reduced by 8.5% ( $SD = 13\%$ ) after the intervention. Fibre-type specific analysis of DiaMin revealed only a significant reduction ( $P = 0.031$ ) in type I fibre diameter (-11%,  $SD = 14\%$ ). The FCSAs of type I fibres trended ( $P = 0.06$ ) to be reduced following the intervention. Across fibre types, the mean number of CaF decreased significantly ( $P = 0.023$ ) from 4.2 ( $SD = 1.3$ ) to 3.6 ( $SD = 0.6$ ). Capillary density ( $P = 0.16$ ), capillary-to-fibre ratio ( $P = 0.53$ ), fibre-type distribution ( $P = 0.96$ ) and FCSA distribution ( $P = 0.82$ ) remained unaltered. An overview of all biopsy data is presented in Table 1.

### Discussion

The main objective of the present study was to assess whether local blood supply in exercising locomotory muscles is reduced after 8 weeks of local muscle unloading and if so, whether such an impaired blood supply would affect WoRPD in response to an incremental isokinetic exercise test. In

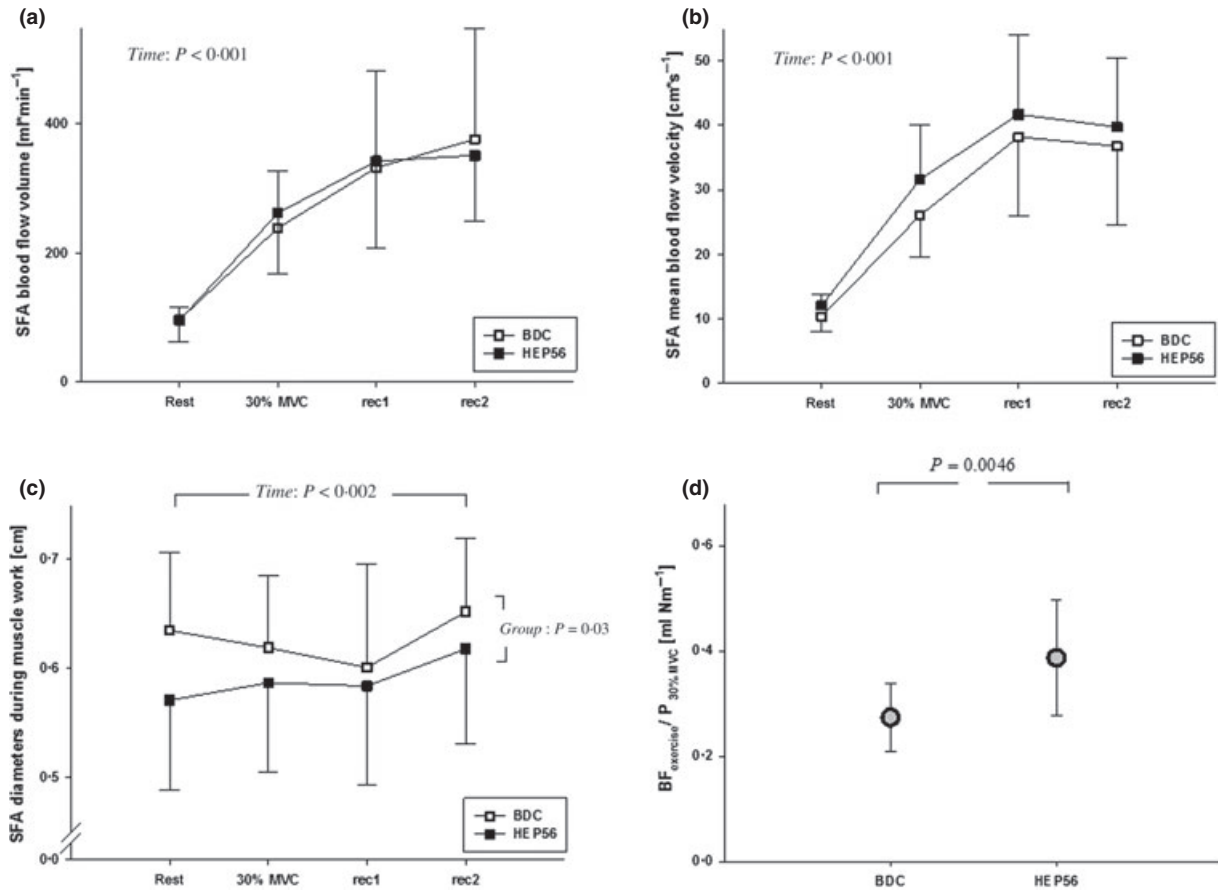


**Figure 5** Arterial blood flow. (a) Absolute blood flow was not different between BDC and HEP56 for all conditions ( $P = 0.95$ ). Within the IJET, blood flow, mean flow velocity (b) and SFA diameters (c) increased significantly over time and absolute arterial diameters were significantly smaller at HEP56 ( $P = 0.03$ ). Panel (d) shows that the ratio of mean blood flow at 30% MVC ( $BF_{\text{exercise}}$ ) and the corresponding plantar flexor power was significantly ( $P = 0.0046$ ) higher at HEP56.

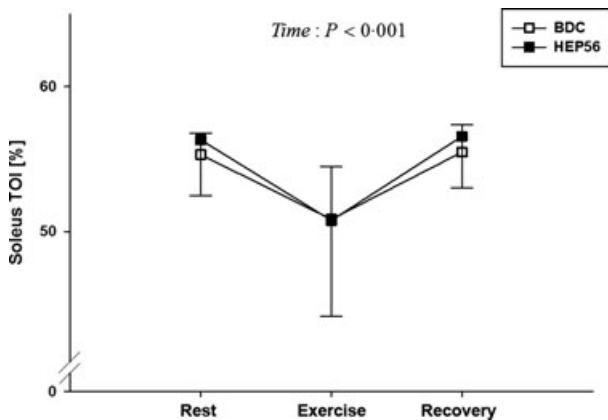


**Figure 6** Soleus muscle tissue oxygenation. Soleus muscle TOI did not change significantly after the intervention ( $P = 0.65$ ). In response to the IJET soleus muscle, TOI decreased significantly ( $P < 0.001$ ) from 55.8% (SD = 2.9%) at rest to 50.8% (SD = 5.2%) during exercise.

contrast to our expectations and in contrast to previous observations (Mulder et al., 2007), the results of this study suggest that local arterial exercise blood flow in the atrophied soleus muscle was maintained after 8 weeks of muscle disuse. Furthermore,

despite the slight reduction of capillaries around fibres, local tissue oxygenation, as assessed by near-infrared spectroscopy did not change nor was the intrinsic WoRPD of the plantar flexor muscle group affected by 8 weeks unloading.

### Muscle performance

Maximal voluntary plantar flexor torque decreased significantly after the intervention. The 23.4% loss of maximal plantar flexor torque at HEP56 is greater than what can be attributed to mere atrophy of soleus muscle fibres, which seems to be a generic finding of unloading studies (Zange et al., 1997; Alkner & Tesch, 2004; Mulder et al., 2006). However, WoRPD, expressed as the relative power difference from MVC1–MVC5 to MVC\_R throughout the IJET protocol (Fig. 4c), remained unaltered. Moreover, lactate concentrations that can be used as an indication for exercise-induced muscle fatigue (Finsterer, 2012) increased equally at BDC and at HEP56, reinforcing notion of an unchanged fatigability after the intervention. The concomitantly obtained EMG recordings also support this notion, as subjects did not show typical electrophysiological symptoms of increased muscle fatigue



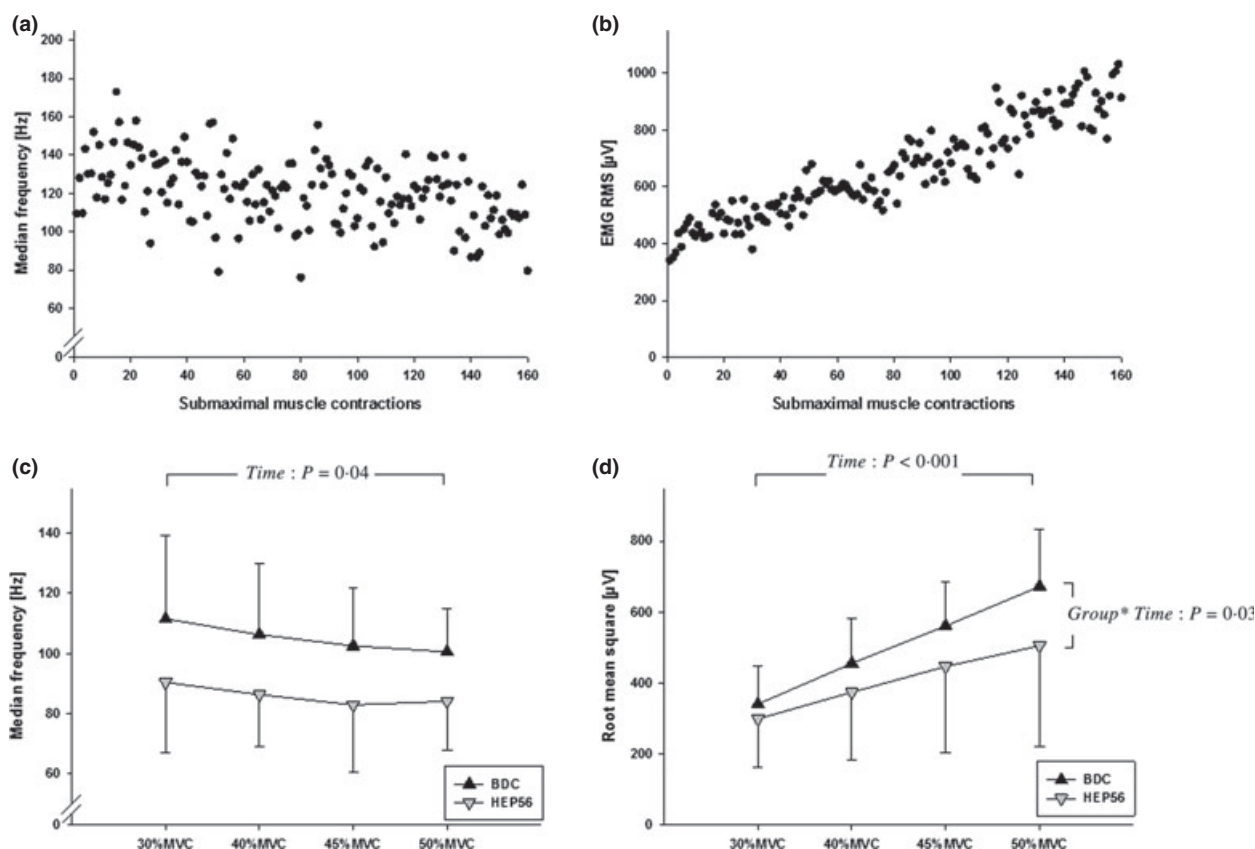


**Figure 7** Soleus muscle electromyography. Shown are MF and RMS values that were calculated for each of the 160 submaximal plantar flexions. Panels (a) and (b) depict exemplary MF and RMS values for one subject. Panels (c) and (d) depict mean MF and RMS values for each stage. MF decreased significantly from stage to stage ( $P = 0.04$ ) while the significant increase of RMS from stage to stage appeared to be more pronounced in response to the BDC IET ( $P = 0.03$ ).

**Table 1** Soleus muscle morphology.

|                                  | Overall          | Type I           | Type II          |
|----------------------------------|------------------|------------------|------------------|
| DiaMin pre [ $\mu\text{m}$ ]     | 71 $\pm$ 13      | 68 $\pm$ 11      | 75 $\pm$ 15      |
| DiaMin post [ $\mu\text{m}$ ]    | 65 $\pm$ 8.5     | 61 $\pm$ 7.7     | 69 $\pm$ 7.5     |
| P-value                          | 0.016            | 0.031            | 0.21             |
| FCSA pre [ $\mu\text{m}^2$ ]     | 14592 $\pm$ 5412 | 12939 $\pm$ 4955 | 16244 $\pm$ 5562 |
| FCSA post [ $\mu\text{m}^2$ ]    | 12381 $\pm$ 3642 | 10202 $\pm$ 2790 | 14561 $\pm$ 3101 |
| P-value                          | 0.06             | 0.06             | 0.40             |
| CaF pre                          | 4.2 $\pm$ 1.3    | 4.2 $\pm$ 1.3    | 4.2 $\pm$ 1.4    |
| CaF post                         | 3.6 $\pm$ 0.6    | 3.6 $\pm$ 0.6    | 3.5 $\pm$ 0.6    |
| P-value                          | 0.023            | 0.15             | 0.10             |
| CD [ $\text{nC mm}^{-2}$ ]       | 289 $\pm$ 123    | —                | —                |
| CD [ $\text{nC mm}^{-2}$ ]       | 229 $\pm$ 54     | —                | —                |
| P-value                          | 0.16             | —                | —                |
| C:F pre [nC/nF]                  | 2 $\pm$ 0.7      | —                | —                |
| C:F post [nC/nF]                 | 1.9 $\pm$ 0.7    | —                | —                |
| P-value                          | 0.53             | —                | —                |
| Fibre type distribution pre [%]  | —                | 68.4 $\pm$ 21.9  | 31.6 $\pm$ 21.9  |
| Fibre type distribution post [%] | —                | 68.7 $\pm$ 12    | 31.3 $\pm$ 12    |
| P-value                          | —                | 0.96             | 0.96             |
| FCSA distribution pre [%]        | —                | 64 $\pm$ 22.9    | 36 $\pm$ 22.9    |
| FCSA distribution post [%]       | —                | 62.6 $\pm$ 13.7  | 37.4 $\pm$ 13.7  |
| P-value                          | —                | 0.82             | 0.82             |

following disuse, which would be indicated by more distinct RMS increases and more pronounced MF decreases in response to exercise (Masuda et al., 1999; Hunter & Enoka, 2003). On the contrary, the amplitude of soleus muscle EMG during the submaximal muscle contractions increased less steeply after the study, which indicates that even less central drive was needed during the post-HEPHAISTOS IIET (Mulder et al., 2007). The trend that overall MFs appeared to be reduced after the study is in agreement with a previous study, where MFs of the vastus lateralis muscle were consistently reduced after 56 days of bed rest in response to an isometric incremental exercise test (Mulder et al., 2009). The decrease in MF reflects most likely a reduction of muscle FCSA as thinner muscle fibres, if compared to thicker fibres, have a reduced conduction velocity (Blijham et al., 2006) that is accompanied by a reduced initial median frequency of the EMG power spectrum (Arendt-Nielsen & Mills, 1985). This endorses the morphological finding of the present study that soleus muscle fibres atrophied after 56 days HEPHAISTOS unloading. It could be argued here that the HEPHAISTOS did not entirely unload calf muscles during gait and that therefore muscle atrophy occurred without inducing any changes of fibre-type distribution that can be observed in conditions associated with complete muscle silencing (Burnham et al., 1997). However, this remains speculative as it is unknown to what degree muscles need to be silenced to evoke fibre-type transformations and it is also possible that 8 weeks of muscle unloading were simply too short to induce such a change (Burnham et al., 1997). Accordingly, the absence of a fibre-type transformation towards glycolytic type II fibres might have contributed to an unchanged WoRPD after the intervention.

### Arterial structure and function

The structural and functional artery adaptations at rest, following 8 weeks of HEPHAISTOS unloading have been published elsewhere (Weber et al., 2013). Those data revealed that resting SFA blood flow did not change after the intervention, despite an average 12.7% (SD = 6.6%) decrease in SFA calibres at rest. This observation is in corroboration with previous unloading studies (De Groot et al., 2004; Bleeker et al., 2005a, b). However, the focus of the present study was on blood flow during exercise, and to the best of our knowledge, there are no disuse studies available to date, that investigated this. The presented data show that absolute arterial exercising blood flow remained unaltered after 56 days of HEPHAISTOS unloading. In fact, the peak SFA blood flow ( $BF_{rec2}$ ) was equally increased from resting conditions to  $364 \text{ ml min}^{-1}$  (SD =  $139 \text{ ml min}^{-1}$ ) before and after the 56 days of unloading. As SFA diameters were significantly smaller at HEP56, an unchanged blood flow must have been compensated by an increased  $V_{mean}$ . At least visually, the data depicted in Fig. 4b seem to corroborate that  $V_{mean}$  is consistently greater at HEP56 when compared with BDC. However, statistically, this difference failed to reach significance. Of note, the postexercise

dilation of 5.8% is in accordance with the magnitude of flow-mediated dilation (FMD) that was measured in the same study (Weber et al., 2013). The latter finding suggests that fatiguing, although submaximal exercise does not cause maximal vasodilation of conduit arteries to supply working muscles with blood, as previous studies showed that the FMD response does not represent maximal dilation capacity (Bleeker et al., 2005b). Considering the above, it seems to be plausible that the unchanged WoRPD can be attributed to the unchanged arterial blood flow, as previous studies related exercise-induced muscle fatigability to mainly resynthesis of phosphocreatine (PCr) that was found to be strongly linked to muscle blood flow (Zange et al., 2008). However, it needs to be stated here that calf muscles constitute only a comparable small muscle mass and it could be argued if blood flow changes might occur when larger muscle volumes are involved. The finding that the arterial diameter did apparently not reach its maximal dilation capacity during the IIET might thus also be attributed to the relatively small volume of the working muscles.

### Tissue oxygenation and blood supply

During muscle work, the tissue oxygenation index (TOI) represents a dynamic balance of oxygen consumption and oxygen delivery (Boushel & Piantadosi, 2000). The presented NIRS data reveal that soleus muscle tissue oxygenation was similar at BDC and HEP56. This finding suggests that blood supply to working muscles was not compromised at HEP56, as one would expect greater oxygen desaturation in poorly perfused muscles (Mulder et al., 2007). The latter is reinforced by the discovery that  $C/F$  was unaffected, because the same diffusion area for oxygen was available after the study. The fact that fibre-type distribution did not change after the 56-day intervention is also in agreement with the unchanged oxygen desaturation during muscle work, as oxygen consumption is dependent on oxidative capacity which in turn is thought to be largely dependent on fibre types (Takekura & Yoshioka, 1987). Albeit the marginal disadvantageous reduction of CaF and with regard to the atrophy of type I fibres, oxygen delivery to the working muscle might even have improved after the intervention as diffusion distances from capillaries to muscle mitochondria should have decreased. Nonetheless, the finding that blood lactate concentrations were similar between experiments, although absolute muscle work was reduced at HEP56, could indicate that the atrophied muscles relied more on glycolysis.

The ratio of blood flow (as measured during the first submaximal stage) and mechanical power (Fig. 5d) suggests a surplus of arterial blood supply after the intervention. As a consequence, HEP56 TOI should be higher than BDC TOI as, with regard to the unchanged capillary-to-fibre ratio, muscle perfusion and therefore oxygen delivery should have been 'luxurious'. Yet, TOI appeared to be similar between BDC and HEP56, suggesting that the muscle was not able to utilize the additional oxygen supplied. It could thus be that the flow that

was going through the SFA did not entirely go through the capillary bed of the soleus muscle, indicating a greater arteriovenous shunt volume after the study. The present findings are somewhat different from what has been found in a previous bed rest study of the same duration (Mulder et al., 2007), where the TOI and the 'blood flow index' as measured with NIRS under administration of indocyanine green were found to be greatly reduced. However, measurement site (soleus versus vastus lateralis), the utilized unloading models and the applied exercise protocols (isokinetic versus isometric intermittent) differed between studies, making it difficult to compare the results.

Furthermore, evidence suggests that reductions of circulating blood greatly contribute to an increased exercise-induced whole body muscle fatigability and a decreased O<sub>2</sub> uptake after periods of bed rest (Convertino, 1997). However, in these all-out exercise tests, exercise-induced muscle fatigability is not normalized for losses of strength or muscle volume. In the present study, we normalized local exercise-induced muscle fatigability for losses of strength, and our data show that after local muscle unloading with HEPHAISTOS where muscles are greatly unloaded but not entirely silenced, blood flow to working muscles is not hindered. On the contrary, blood flow during and after exercise appears to be unaltered, suggesting a 'luxurious' conduit artery blood flow after the intervention. This might imply that peripheral vascular adaptations do not account for the disuse-induced reduction of VO<sub>2</sub> as seen in bed rest, at least during the first 8 weeks.

## Conclusion

The presented results reveal that although maximal plantar flexor strength, soleus muscle fibre size and arterial dimen-

sions decreased significantly, exercising blood flow and tissue oxygenation in the soleus muscle were maintained after 56 days disuse, and even increased when expressed in relative terms. Moreover, and possibly as a consequence of this, the presented data show that the soleus work-related power decrease, as a measure for exercise-induced muscle fatigue, following submaximal muscle work does not change after 56 days of local muscle unloading with HEPHAISTOS, if normalized to maximal muscle strength. The unchanged exercise-induced muscle fatigue is also reflected in the electromyographic activity of the soleus muscle where typical neuronal signs of muscle fatigue were not deteriorated. In a nutshell, the presented data suggest that the actual endurance quality of unloaded soleus muscle tissue does not change and that blood flow and oxygenation in working muscles do not constitute a limiting factor for ongoing submaximal muscle work after 56 days of local muscle unloading.

## Acknowledgments

The authors would like to acknowledge the support of the Space Physiology staff. Particularly, Luis Beck, Pengfei Yang, Vassilis Anagnostou, Christian Schmickler, Izad Bayan Zadeh and Suheip Abu-Nasir should be mentioned here. The first author receives a Helmholtz Space Life Sciences Research School (SpaceLife) scholarship. SpaceLife is funded in equal parts by the Helmholtz Association and the German Aerospace Center (DLR).

## Conflict of interest

The authors have no conflict of interests.

## References

- Alkner BA, Tesch PA. Knee extensor and plantar flexor muscle size and function following 90 days of bed rest with or without resistance exercise. *Eur J Appl Physiol* (2004); **93**: 294–305.
- Arendt-Nielsen L, Mills KR. The relationship between mean power frequency of the EMG spectrum and muscle fibre conduction velocity. *Electroencephalogr Clin Neurophysiol* (1985); **60**: 130–134.
- Berg HE, Dudley GA, Hather B, Tesch PA. Work capacity and metabolic and morphologic characteristics of the human quadriceps muscle in response to unloading. *Clin Physiol* (1993); **13**: 337–347.
- Bleeker MW, De Groot PC, Poelkens F, Rongen GA, Smits P, Hopman MT. Vascular adaptation to 4 wk of deconditioning by unilateral lower limb suspension. *Am J Physiol Heart Circ Physiol* (2005a); **288**: H1747–H1755.
- Bleeker MW, De Groot PC, Rongen GA, Rittweger J, Felsenberg D, Smits P, Hopman MT. Vascular adaptation to deconditioning and the effect of an exercise countermeasure: results of the Berlin Bed Rest study. *J Appl Physiol* (2005b); **99**: 1293–1300.
- Blijham PJ, ter Laak HJ, Schelhaas HJ, van Engelen BG, Stegeman DF, Zwartz MJ. Relation between muscle fiber conduction velocity and fiber size in neuromuscular disorders. *J Appl Physiol* (2006); **100**: 1837–1841.
- Boushel R, Piantadosi CA. Near-infrared spectroscopy for monitoring muscle oxygenation. *Acta Physiol Scand* (2000); **168**: 615–622.
- Bremser M, Mittag U, Weber T, Rittweger J, Herpers R. Diameter measurement of vascular structures in ultrasound video sequences. In: *Bildverarbeitung für die Medizin 2012* (eds Tolxdorff, T, Deserno, TM, Handels, H, Meinzer, HP) (2012), pp. 165–170. Springer, Berlin, Heidelberg.
- Brooke MH, Kaiser KK. Muscle fiber types: how many and what kind? *Arch Neurol* (1970); **23**: 369–379.
- Burnham R, Martin T, Stein R, Bell G, MacLean I, Steadward R. Skeletal muscle fibre type transformation following spinal cord injury. *Spinal Cord* (1997); **35**: 86–91.
- Convertino VA. Cardiovascular consequences of bed rest: effect on maximal oxygen uptake. *Med Sci Sports Exerc* (1997); **29**: 191–196.
- De Groot PC, Poelkens F, Kooijman M, Hopman MT. Preserved flow-mediated dilation in the inactive legs of spinal cord-injured individuals. *Am J Physiol Heart Circ Physiol* (2004); **287**: H374–H380.
- De Groot PC, Bleeker MW, van Kuppevelt DH, van der Woude LH, Hopman MT.

- Rapid and extensive arterial adaptations after spinal cord injury. *Arch Phys Med Rehabil* (2006); **87**: 688–696.
- Degens H, Alway SE. Control of muscle size during disuse, disease, and aging. *Int J Sports Med* (2006); **27**: 94–99.
- Deschenes MR, Giles JA, McCoy RW, Volek JS, Gomez AL, Kraemer WJ. Neural factors account for strength decrements observed after short-term muscle unloading. *Am J Physiol Regul Integr Comp Physiol* (2002); **282**: R578–R583.
- Enoka RM, Duchateau J. Muscle fatigue: what, why and how it influences muscle function. *J Physiol* (2008); **586**: 11–23.
- Finsterer J. Biomarkers of peripheral muscle fatigue during exercise. *BMC Musculoskelet Disord* (2012); **13**: 218.
- Geraskin D, Boeth H, Kohl-Bareis M. Optical measurement of adipose tissue thickness and comparison with ultrasound, magnetic resonance imaging, and callipers. *J Biomed Opt* (2009); **14**: 044017.
- Hunter SK, Enoka RM. Changes in muscle activation can prolong the endurance time of a submaximal isometric contraction in humans. *J Appl Physiol* (2003); **94**: 108–118.
- Huonker M, Schmid A, Schmidt-Trucksass A, Grathwohl D, Keul J. Size and blood flow of central and peripheral arteries in highly trained able-bodied and disabled athletes. *J Appl Physiol* (2003); **95**: 685–691.
- Koryak Y. Changes in the action potential and contractile properties of skeletal muscle in human's with repetitive stimulation after long-term dry immersion. *Eur J Appl Physiol Occup Physiol* (1996); **74**: 496–503.
- Masuda K, Masuda T, Sadoyama T, Inaki M, Katsuta S. Changes in surface EMG parameters during static and dynamic fatiguing contractions. *J Electromyogr Kinesiol* (1999); **9**: 39–46.
- Mulder ER, Stegeman DF, Gerrits KH, Paalman MI, Rittweger J, Felsenberg D, de Haan A. Strength, size and activation of knee extensors followed during 8 weeks of horizontal bed rest and the influence of a countermeasure. *Eur J Appl Physiol* (2006); **97**: 706–715.
- Mulder ER, Kuebler WM, Gerrits KH, Rittweger J, Felsenberg D, Stegeman DF, de Haan A. Knee extensor fatigability after bedrest for 8 weeks with and without countermeasure. *Muscle Nerve* (2007); **36**: 798–806.
- Mulder ER, Gerrits KH, Kleine BU, Rittweger J, Felsenberg D, de Haan A, Stegeman DF. High-density surface EMG study on the time course of central nervous and peripheral neuromuscular changes during 8 weeks of bed rest with or without resistive vibration exercise. *J Electromyogr Kinesiol* (2009); **19**: 208–218.
- Portero P, Vanhoutte C, Goubel F. Surface electromyogram power spectrum changes in human leg muscles following 4 weeks of simulated microgravity. *Eur J Appl Physiol Occup Physiol* (1996); **73**: 340–345.
- de Ruiter CJ, Goudsmit JF, Van Tricht JA, de Haan A. The isometric torque at which knee-extensor muscle reoxygenation stops. *Med Sci Sports Exerc* (2007); **39**: 443–453.
- Semmler JG, Kutzscher DV, Enoka RM. Limb immobilization alters muscle activation patterns during a fatiguing isometric contraction. *Muscle Nerve* (2000); **23**: 1381–1392.
- Shaffer MA, Okereke E, Esterhai JL Jr, Elliott MA, Walker GA, Yim SH, Vandenborne K. Effects of immobilization on plantar-flexion torque, fatigue resistance, and functional ability following an ankle fracture. *Phys Ther* (2000); **80**: 769–780.
- Sugawara J, Hayashi K, Kaneko F, Yamada H, Kizuka T, Tanaka H. Reductions in basal limb blood flow and lumen diameter after short-term leg casting. *Med Sci Sports Exerc* (2004); **36**: 1689–1694.
- Takekura H, Yoshioka T. Determination of metabolic profiles on single muscle fibres of different types. *J Muscle Res Cell Motil* (1987); **8**: 342–348.
- Thijssen DH, Maiorana AJ, O'Driscoll G, Cable NT, Hopman MT, Green DJ. Impact of inactivity and exercise on the vasculature in humans. *Eur J Appl Physiol* (2010); **108**: 845–875.
- Trappe S, Trappe T, Gallagher P, Harber M, Alkner B, Tesch P. Human single muscle fibre function with 84 day bed-rest and resistance exercise. *J Physiol* (2004); **557**: 501–513.
- Weber T, Ducos M, Mulder E, Herrera F, Bruggemann GP, Bloch W, Rittweger J. The specific role of gravitational accelerations for arterial adaptations. *J Appl Physiol* (2013); **114**: 387–393.
- Witzmann FA, Kim DH, Fitts RH. Effect of hindlimb immobilization on the fatigability of skeletal muscle. *J Appl Physiol* (1983); **54**: 1242–1248.
- Zange J, Muller K, Schuber M, Wackerhage H, Hoffmann U, Gunther RW, Adam G, Neuerburg JM, Sinitsyn VE, Bacharev AO, Belichenko OI. Changes in calf muscle performance, energy metabolism, and muscle volume caused by long-term stay on space station MIR. *Int J Sports Med* (1997); **18** (Suppl 4): S308–S309.
- Zange J, Beisteiner M, Muller K, Shushakov V, Maassen N. Energy metabolism in intensively exercising calf muscle under a simulated orthostasis. *Pflugers Arch* (2008); **455**: 1153–1163.